# THERMAL CONDUCTIVITY OF POLYIMIDE/CARBON NANOFILLER BLENDS

**D.M. Delozier[1], K.A. Watson[1], S. Ghose[2], D.C. Working[3], J.W. Connell[3], J.G. Smith[3], Y.P. Sun[4] and Y. Lin[4]**

[1] National Institute of Aerospace, Hampton, VA 23666-6147

[2]National Research Council Associate at NASA LaRC, Hampton, VA 23681

[3]NASA Langley Research Center, Hampton, VA 23681-2199

[4]Dept of Chemistry, Clemson University, Clemson, SC 26934-0973

E-mail: d.m.delozier@larc.nasa.gov

**Keywords**
Thermal Conductivity, Nanofillers, Polyimide

## INTRODUCTION

Combining polymers with an organic or inorganic filler to produce a polymer composite is common in the production and processing of modern plastics. Recently, filler sizes have been reduced to nanometer dimensions resulting in a new class of materials termed polymer nanocomposites (PNC). PNCs are commonly defined as the combination of a polymer matrix resin with inclusions that have at least one dimension in the nanometer size range [i]. PNCs exhibit significant enhancements in certain properties at a far lower concentration than their conventional micro or macro counterparts. Layered clay, expanded graphite, carbon nanofibers and carbon nanotubes are some of the common nanoparticles used in making PNCs.

Carbon nanofibers (CNF) are widely used as reinforcements for polymers in numerous high-technology applications because of their excellent electrical and thermal properties and high specific tensile strength and modulus [ii]. These highly graphitic fibers are produced by a catalytic vapor deposition process and have a wide range of morphologies, from disordered bamboo-like formations [iii] to highly graphitized "stacked-cup" structures where conical shells are nested within one another [iv]. Although CNFs are not naturally occurring they are economically attractive when compared with other synthetically produced carbon forms such as carbon nanotubes. CNFs have been used as reinforcements for various thermoplastics like polyethylene [v], polypropylene [vi,vii], polycarbonate [viii], nylon [ix] and poly (methyl methacrylate) [x]. PNCs containing CNFs can have altered properties including improved heat distortion temperatures and increased electromagnetic shielding.

Graphite is another material that is commonly used as a filler in polymers. Graphite is one of the stiffest naturally occurring materials with a Young's modulus of ~1060 MPa and also has excellent thermal and electrical conductivity. In addition, the material is presently two orders of magnitude less expensive than carbon nanotubes [xi].Utilizing natural graphite, which exists in large stacks of graphene sheets, necessitates expansion and exfoliation of the graphene layers to obtain particles with nanometer dimensions. Graphite can be expanded via known processes and the resulting expanded graphite (EG) is more easily dispersed in a polymer matrix. The resulting EG PNCs can have greatly improved mechanical and

electrical properties and high thermal conductivity when compared to their unfilled counterparts. Electrically conductive nanocomposites were prepared by solution intercalation and master batch melt mixing of high density polyethylene (HDPE)/maleic anhydride grafted polyethylene and expanded graphite [xii]. HDPE was also reinforced with EG and untreated graphite by a melt compounding process that improved electrical and mechanical properties of the EG system [xiii]. Poly(styrene-co-acrylonitrile)/EG composite sheets [xiv], polymethylmethacrylate/EG composites prepared by solution blending methods [xv], and aromatic polydisulphide/EG nanocomposites prepared by solution method and hot molding [xvi] which showed good mechanical and electrical properties are other examples of EG containing PNCs. The dynamic mechanical and thermal properties of phenylethynyl-terminated polyimide composites reinforced with EG nanoplatelets have also been studied [xvii].

Carbon nanotube (CNT) based composites are being widely studied due to the unique physical/mechanical properties of CNTs. CNTs are thought of as the ultimate carbon fiber, and computer modeling predicts them to have high mechanical and electrical properties and ultra high thermal conductivity [xviii, xix]. When CNTs are dispersed in polymeric materials, an interconnecting network is usually formed which provides a conductive pathway for electrical and/or thermal current to flow. In electrical conductivity the mechanism involves a flow of electrons whereas for thermal conductivity the process of conduction occurs via transfer of phonons. Various methods have been attempted for achieving good dispersion of CNTs in the polymer. They include the preparation of the polymer in the presence of CNTs under sonication [xx], the use of alkoxysilane terminated amide acid oligomers to disperse the CNTs [xxi], melt mixing [xxii] and shear mixing [xxiii]. Theory predicts the thermal conductivity of carbon nanotubes at room temperature is as high as ~6600 W/mK [xxiv]. The experimental value of 3000 W/mK for the thermal conductivity of an individual multiwalled carbon nanotube (MWCNT) at room temperature has been reported [xxv]. This value is significantly higher than that of known thermally conducting materials like diamond (up to 2300 W/mK) and graphite (up to 1960 W/mK). The prominent thermal properties of CNTs have made them promising materials for future applications as thermal management materials. Enhancement of thermal conductivity has been observed in CNT suspensions [xxvi-xxvii]. It is interesting to note that in the case of CNT suspensions, the measured thermal conductivities are generally lower than the theoretical predictions made with conventional heat conduction models. It has been shown in the case of single wall carbon nanotubes (SWCNTs) that thermal conductivities show a peaking behavior before falling off at higher temperatures due to Umklapp scattering [xxviii]. In the case of ordinary carbon-carbon composites, there is larger mean free path and less phonon-phonon Umklapp scattering causing the thermal conductivity to increase linearly with heat treatment temperature [xxix]. However, in PNCs, the improvement in thermal conductivity has always been lower than the predicted rule-of-mixture values.

In efforts to improve the TC of various components of the liquid cooling ventilation garment in the spacesuit, polymer samples containing the various fillers at representative loading levels were prepared. ULTEM™ was initially chosen for use as the host resin because the resin is an amorphous thermoplastic polyetherimide offering good melt processability, outstanding high heat resistance, high strength, modulus and broad chemical resistance. Although ULTEM™ is not used in the spacesuit the TC properties are expected to be very similar in any polymer system. Recently SWCNTs were incorporated (up to 1% by weight)

into ULTEM™ and melt processed to yield fibers which offered some initial parameters for this work [xxx]. Although the melt process was not optimized to fully disperse and align the SWCNTs some improvements in mechanical properties were achieved.

Melt compounding was chosen as the method to disperse the nanoparticles in ULTEM™ because it involves high shear mixing which helps to disentangle the nanoparticles and disperse them uniformly within the matrix. Melt mixing was followed by extrusion in the preparation of some of the samples described herein as the process of extruding the nanocomposite through a suitable die and subsequent drawing led to continuous ribbons of nanocomposites with substantial orientation of the nanoparticles in the flow direction. The samples were characterized using differential scanning calorimetry (DSC), thermogravimetric analysis (TGA), high resolution scanning electron microscopy (HRSEM), mechanical tester and thermal conductivity analyzer. The preparation and characterization of samples containing various loadings of CNTs, CNFs and EGs are discussed.

## EXPERIMENTAL

**Materials** Ultem™ 1000, a melt processable polyimide, was obtained from GE Plastics and used as received. MWCNTs, VGE-S16, were procured from the University of Kentucky. CNF, Pyrograph – III - PR-24 HHT, was obtained from Applied Sciences, Inc and EG was received from Asbury Carbons. The graphite already had the galleries expanded by first treating with sulfuric acid and then rapidly heating the sample to 900 ºC. The expansion of the graphite was expected to facilitate exfoliation during melt mixing.

**Processing of Ultem™ 1000 with Nanofillers** Ultem™ 1000 was compounded with MWCNTs, CNFs and EGs in a 30 cc internal mixer (Plasticorder PL2000, Banbury) for 3 h at 25 rpm, 325 °C under $N_2$ purge. MWCNTs - 5, 10 and 20 wt%, CNFs - 20, 30 and 40 wt%, and EGs - 20, 30, 40 and 50 wt% were added to the polymer. During mixing the torque produced was used to calculate the viscosity of the sample. Upon completion of mixing the material was ground in a Mini-Granulator (Kayeness, Inc) using a 5.5 mm screen. Samples were extruded through a Laboratory Mixing Extruder (#LME, Dynisco, Inc) at a barrel temperature of 215 °C and a die temperature of 365 °C for the CNF sample, a barrel temperature of 215 °C and a die temperature of 360 °C for the MWCNT sample and a barrel temperature of 190 °C and a die temperature of 350 °C for the EG sample. The dimensions of the die were 0.38 mm x 19.1 mm. The samples were extruded in the form of a continuous ribbon that were 0.1-0.5 mm thick, 10-15 mm wide and several meters in length. Once extruded, the ribbons were cut into pieces approximately 2 cm x 2 cm. They were then stacked on one side of a mold 9 cm x 2 cm x 3 cm (i.d.) and the remainder of the mold filled with Ultem™ pellets. The stacked ribbons were compression molded at 270 °C, 1.72 MPa for 3 h. The molded samples were then sliced using an Isomet low speed saw with a diamond wafering blade 10.2 cm diameter and 0.3 mm thick with 15 HC diamond (Buehler Ltd). Unoriented samples were made using a Laboratory Mixing Molder (#LMM Dynisco, Inc) and a rectangular mold (1.52 mm x 38.1 mm x 1.27 mm). A rough blend of materials was added to the mixing bowl of LMM kept at 360 $^{o}$C and kept there for 0.5 h. It was then dynamically pressed at a rotational speed of 100% of ram-motor capacity and then static pressed to degas, before passing through the nozzle orifice (~1.6 mm) into the rectangular mold kept at 360 $^{o}$C. The material was then manually compressed at a pressure of ~ 4.5 kN and set under pressure from the ram while being air cooled.

**Characterization** DSC was performed on the ribbon samples obtained from extrusion in a sealed aluminum pan using a Shimadzu DSC-50 thermal analyzer at a heating rate of 20 $^{o}$C/min with the glass transition temperature ($T_g$) taken as the mid-point of inflection of the differential heat flow ($\Delta H$) versus temperature curve. TGA was performed in air (flow rate – 50 mL/min) on the powder samples using an Auto TGA 2950HR (TA Instruments, DE). The samples were heated at 20 $^{o}$C/min to 100 $^{o}$C, held for 0.5 h to drive off any moisture, and heated to 600 $^{o}$C at a rate of 2.5 $^{o}$C/min. HRSEM images were obtained using a Hitachi S-5200 field emission scanning electron microscope equipped with a "through-the-lens" secondary electron detector. Thin-film tensile properties were determined according to ASTM D882 using either four or five specimens (0.51 cm wide) per test conditions using an Eaton Model 3397-139 11.4 kg load cell on a Sintech 2 test frame. The test specimen gauge length was 5.1 cm and the crosshead speed for film testing was 0.51 cm/minute. Thermal conductivity of the molded samples as well as ribbons was measured using a Netzsch LFA 447 NanoFlash according to ASTM E1461. Samples sizes of 1 cm x 1 cm were sprayed with a thin layer of graphite (for uniform thermal adsorption), which may be easily rinsed away by solvent (e.g., methanol). Pyrex (TC ~ 1.09 W/mK, Cp ~ 0.76 J/gk) was used as the reference.

## RESULTS AND DISCUSSION

**Processing of Ultem™/Nanofillers** Torque values were obtained during mixing in the Plasticorder and were used to calculate the melt viscosities of the samples. Table 1 denotes the calculated melt viscosities of the various samples at a shear rate of 92.5 sec$^{-1}$ and a temperature of 325 ° C.

Table 1: Melt viscosities of Ultem™ 1000/nanofiller samples: Shear rate: 92.5/sec, Temperature: 325 $^{o}$C

| Sample | Viscosity (poise) |
|---|---|
| Neat Ultem™ | 37200 |
| Ultem™, 5 wt% MWCNTs | 38000 |
| Ultem™, 10 wt% MWCNTs | 47700 |
| Ultem™, 20 wt% MWCNTs | 54700 |
| Ultem™, 20 wt% CNFs | 35400 |
| Ultem™, 30 wt% CNFs | 47200 |
| Ultem™, 40 wt% CNFs | 50300 |
| Ultem™, 20 wt% EGs | 31500 |
| Ultem™, 30 wt% EGs | 37000 |
| Ultem™, 40 wt% EGs | 46800 |
| Ultem™, 50 wt% EGs | 57800 |

It was found that some samples (40 wt% CNF, 50 wt% EG) could not be extruded into ribbons. The difficulty in extruding these samples could be attributed to either their high melt viscosity or increased thermal conductivity. A large increase in thermal conductivity would lead to additional heating in the feeding region of the extruder which would prevent the material from exiting properly. Figure 1 shows a picture of a typical extruded ribbon.

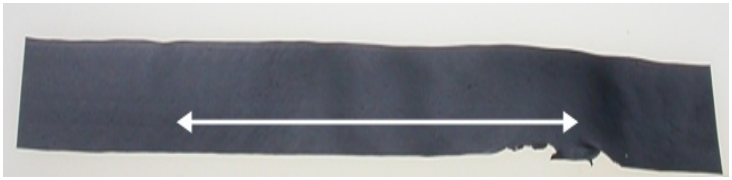

Figure 1. Ribbon of Ultem™/MWCNTs with arrow showing direction of tube alignment

Alignment of the nanofillers in the direction of flow was expected as a result of the extrusion process. In efforts to measure the TC in the direction of the expected alignment, small pieces of the ribbons were stacked in the same direction and pressed together while heating. The molded samples that were obtained were further processed by cutting the molded block in the direction opposite of the alignment using a diamond saw. Thus, samples were obtained with nanofillers alignment both parallel (molded) and perpendicular (ribbon) to the direction of the thermal conductivity measurement.

HRSEM images of extruded ribbons (Figure 2) shows orientation of the MWCNTs, CNFs, and EG along the direction of extrusion.

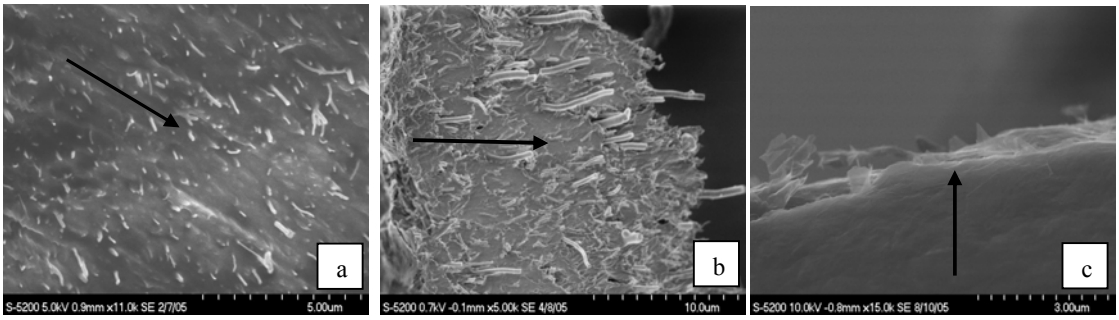


Figure 2: HRSEM images of a) MWCNTs b) CNF and c) EG ribbon samples; arrow denotes direction of flow

It is more difficult to assign directionality to a rectangular sheet, but the EG sheets appear to be in the same planar arrangement as a result of extrusion. The platelets are well dispersed throughout the polymer and are typically smaller than 1 micron in any dimension. The platelets also appear to be very thin which indicates that exfoliation is taking place during the melt mixing and/or extrusion.

**Mechanical Properties of Extruded Ribbons** Mechanical properties were measured on Ultem™/nanofiller composites with the results shown in Table 2.

Table 2: Mechanical properties of Ultem™/nanofiller samples

| **Sample** | **Modulus, GPa** | **Strength, MPa** | **Elongation, %** |
|---|---|---|---|
| Ultem™ -- Neat | 1.45 ± 0.05 | 49.64 ± 1.38 | 16 ± 11 |
| Ultem™, 5 wt% MWCNT, melt | 2.56 ± 0.12 | 91.70 ± 6.20 | 7 ± 0.5 |
| Ultem™, 10 wt% MWCNT, melt | 2.95 ± 0.17 | 72.39 ± 5.51 | 4 ± 1 |
| Ultem™, 20 wt% MWCNT, melt | 3.50 ± 0.30 | 60.67 ± 11.72 | 2 ± .4 |
| Ultem™, 20 wt% CNF, melt | 2.83 ± 0.30 | 48.26 ± 6.89 | 2 ± 0.3 |
| Ultem™, 30 wt% CNF, melt | 3.76 ± 0.16 | 78.60 ± 5.52 | 3 ± 0.6 |
| Ultem™, 20 wt% EG, melt | 5.40 ± 0.2 | 80.00 ± 13.00 | 2 ± 0.4 |
| Ultem™, 30 wt% EG, melt | 7.6 ± 0.3 | 96.5 ± 19.00 | 2 ± 0.5 |

The strips used for testing were cut from ribbons that were prepared by the extrusion process; hence the nanofillers are somewhat aligned in the direction of the strain. The 40 wt% EG

melt mixed sample did not provide ribbons of sufficient quality for mechanical testing. The other results should be viewed with care because the measurement of the ribbon thickness may not be accurate due to uneven ribbon surfaces. As is typically found with filled systems with increased filler loading level the modulus increased and the elongation decreased.

**Thermal Characterization of Extruded Ribbons** The glass transition temperatures ($T_g$) of the various samples are recorded in Table 3.

Table 3: Glass transition temperature ($T_g$) of Ultem™/nanofiller samples

| **Sample** | **Melt mixed, $T_g$ (°C)** |
|---|---|
| Ultem™, neat | 216 (no mixing for neat) |
| Ultem™, 5 wt% MWCNT | 217 |
| Ultem™, 10 wt% MWCNT | 218 |
| Ultem™, 20 wt% MWCNT | 218 |
| Ultem™, 20 wt% CNF | 219 |
| Ultem™, 30 wt% CNF | 218 |
| Ultem™, 20 wt% EG | 218 |
| Ultem™, 30 wt% EG | 219 |
| Ultem™, 40 wt% EG | 219 |

In all the samples very little change in $T_g$ was witnessed. The addition of nanofillers improved the temperature of 5 wt% loss as determined by TGA. Neat Ultem™ lost 5 wt% at ~ 480 °C while the filled samples lost the same weight at temperatures > 500 °C. No significant differences in thermo-oxidative stability were observed for the melt-mixed samples.

**Thermal Conductivity Measurements** Since the structure of nanotubes is anisotropic, the electrical and thermal properties should be different in the longitudinal (parallel to nanotube axis) and transverse (perpendicular to nanotube axis) directions. There have been reports on the use of dispersed CNTs as thermally conducting fillers in polymer composites and certain enhancements in thermal conductivity were observed [xxiv, xxxi]. However, the enhanced values are typically below those predicted by the rule of mixtures. One probable reason for this is the existence of interface thermal resistance between the CNTs leading to an increase in overall thermal resistance [xxxii]. Huang et al. [xxxi] proposed a composite structure where all the CNTs embedded in the matrix are aligned from one surface to the opposite side with all the CNT surfaces revealed on both surfaces. This leads to high thermal conductivity since the CNTs form ideal thermally conducting pathways. Low thermal interface resistances can also be expected as the protruding tips would ensure better thermal contact. Other reports also indicate that alignment of nanofillers in the polymer matrix leads to enhancement of thermal conductivity [xxix, xxxiii]. Based on the literature survey done so far, it was decided to process samples with significant nanofiller alignment and measure thermal conductivity in the direction of alignment and also perpendicular to the direction of alignment for comparison purposes.

Three types of Ultem™/nanofiller samples were measured for thermal conductivity and include the extruded ribbon, molded samples cut perpendicular to flow direction, and samples

with no alignment prepared with the LMM. Table 4a denotes the values for neat Ultem™ and Ultem™/nanofiller ribbon samples.

Table 4a: Thermal conductivity of Ultem™/nanofiller extruded ribbons

| Sample | Thermal Conductivity, W/mK |
|---|---|
| Neat Ultem™ | 0.172 |
| Ultem™, 5 wt% MWCNT, melt | 0.229 |
| Ultem™, 10 wt% MWCNT, melt | 0.272 |
| Ultem™, 20 wt% MWCNT, melt | 0.389 |
| Ultem™, 20 wt% CNF, melt | 0.364 |
| Ultem™, 30 wt% CNF, melt | 0.463 |
| Ultem™, 20 wt% EG, melt | 0.248 |
| Ultem™, 30 wt% EG, melt | 0.287 |
| Ultem™, 40 wt% EG, melt | 0.387 |

In general, the thermal conductivity increased with increase in loading level of nanofillers. The highest thermal conductivity was observed in the 30 wt% CNF samples and the conductivity was increased by 180% with respect to the neat material. The second set of samples was the molded samples where the thermal conductivity was measured in the direction of nanofiller alignment. Table 4b shows the values for the neat molded sample as well as Ultem™/nanofiller samples.

Table 4b: Thermal conductivity of Ultem™/nanofiller molded samples

| Sample | Thermal Conductivity, W/mK |
|---|---|
| Neat Ultem™ | 0.184 |
| Ultem™, 5 wt% MWCNT, melt | 0.592 |
| Ultem™, 10 wt% MWCNT, melt | 1.337 |
| Ultem™, 20 wt% MWCNT, melt | 2.132 |
| Ultem™, 20 wt% CNF, melt | 1.955 |
| Ultem™, 30 wt% CNF, melt | 2.734 |
| Ultem™, 20 wt% EG, melt | 2.956 |
| Ultem™, 30 wt% EG, melt | 4.499 |
| Ultem™, 40 wt% EG, melt | 6.777 |

The thermal conductivity of the samples were observed to be significantly greater in the direction of alignment (Table 4b) compared to those that were perpendicular to the direction of alignment (Table 4a). The MWCNT samples at 20 wt% loading exhibited an 11.5-fold increase in thermal conductivity relative to neat Ultem™ whereas the CNF samples loaded at 30 wt% showed a 15-fold increase. The largest increase was exhibited by 40 wt% loading of EG samples which showed a 38-fold increase. The data indicates that the nanofillers, when aligned, form a network that successfully conducts heat by enabling a more efficient phonon transfer from one filler particle to another. Finally when it comes to the unoriented samples (Table 4c), it was found that 40 wt% CNF filled samples showed a 10-fold increase while the 50 wt% EG sample showed a 19-fold improvement in thermal conductivity.

Table 4c: Thermal conductivity of Ultem™/nanofiller LMM samples (unoriented)

| Sample | Thermal Conductivity, W/mK |
|---|---|

| | |
|---|---|
| Neat Ultem™ | 0.172 |
| Ultem™, 20 wt% MWCNT, melt | 0.500 |
| Ultem™, 40 wt% CNF, melt | 1.184 |
| Ultem™, 20 wt% EG, melt | 0.585 |
| Ultem™, 30 wt% EG, melt | 0.973 |
| Ultem™, 40 wt% EG, melt | 2.144 |
| Ultem™, 50 wt% EG, melt | 3.174 |

The results are graphically depicted in Figure 3.

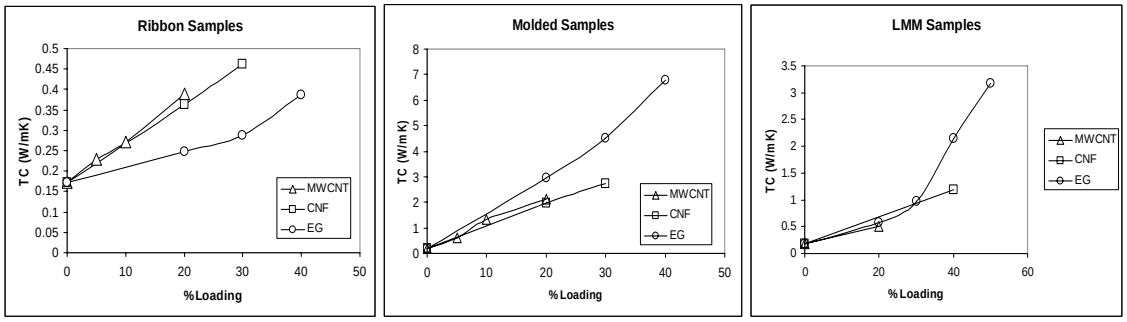


Figure 3. Graphic depiction of TC data.

These results prove conclusively that alignment of the nanofillers in the polymer matrix significantly raises the thermal conductivity of the samples. However, unaligned samples also show a significant improvement and may be useful in applications when it is not possible to achieve nanoparticles alignment in the desired direction.

## SUMMARY

Ultem™ was mixed with three different carbon-based nanofillers in efforts to increase the thermal conductivity of the polymer. After initial mixing, the nanocomposites were extruded or processed via the LMM process. HRSEM revealed significant alignment of the nanofillers in the extruded samples. Thermal conductivity measurements were made both in the direction and perpendicular to the direction of alignment of nanofillers as well as for unaligned samples. It was found that the largest improvement in thermal conductivity was achieved in the case of aligned samples when the measurement was performed in the direction of alignment. Unaligned samples also showed a significant improvement in thermal conductivity and may be useful in applications when it is not possible to align the nanofiller. However the improvements in thermal conductivity did not approach those expected based on a rule of mixtures. This is likely due to poor phonon transfer through the matrix.


### ACKNOWLEDGEMENTS

The authors would like to gratefully acknowledge Prof. Lawrence T. Drzal of Michigan State University for his valuable discussion. They would also like to thank Kevin Bolesta of Asbury Carbons for providing the EG and Tom Hughes of Applied Sciences, Inc. for providing the CNFs.


---


[i]. J. Collister, Polymer Nanocomposites: Synthesis, Characterization and Modeling, Ed. R. Krishnamoorti and R.A. Vaia, ACS Symposium Series 804, (2002).

[ii]. E. Hammel, X. Tang, M. Trampert, T. Schmitt, K. Mauthner, A. Eder and P. Potschke, Carbon, 42, 1153-1158 (2004).

[iii]. V.I. Merkulov, D.H. Lowndes, Y.Y. Wei, G. Eres and E. Voelkl, Appl Phys Lett, 76(24), 3555 (2000).
[iv]. M. Endo, Y.A. Kim, T. Hayashi, Y. Fukai, K. Oshida, M. Terrones, T. Yanagisawa, S. Higaki and M.S. Dresselhaus, Appl Phys Lett, 80(7), 1267 (2002).
[v]. K. Lozano, S. Yang and Q. Zeng, J. Appl. Poly. Sc., 93, 155-162 (2004).
[vi]. R.J. Kuriger, M.K. Alam, D.P. Anderson and R.L. Jacobsen, Composites, Part A, 33, 53-62 (2002).
[vii]. K. Lozano, J. Bonilla-Rios and E.V. Barrera, J. Appl. Poly. Sc., 79, 125-133 (2001).
[viii]. O.S. Carneiro, J.A. Covas, C.A. Bernardo, G. Caldeira, F.W.J. Van Hattum, J.M. Ting, R.L. Alig and M.L. Lake; Composites Sc. Tech., 58, 401-407 (1998).
[ix]. R.T. Pogue, J. Ye, D.A. Klosterman, A.S. Glass and R.P. Chartoff, Composites: Part A, 29, 1273 (1998).
[x]. C.A. Cooper, D. Ravich, D. Lips, J. Mayer and H.D. Wagner, Composites Sc. Tech., 62, 1105 (2002).
[xi]. L.T. Drzal and H. Fukushima, Unites States Patent Application Publication, Pub No. US20040127621 (2004).
[xii]. J.W. Shen, W.Y. Huang, S.W. Zuo and J. Hou, J.Appl. Polym. Sc., 97, 51-59 (2005).
[xiii]. W.Zheng, X. Lu and S.C. Wong, J. Appl. Polym. Sc., 91, 2781-2788, (2004).
[xiv]. G. Zheng, J. Wu, W. Wang and C. Pan, Carbon, 42, 2839-2847 (2004).
[xv]. W. Zheng, S.C. Wong and H.J. Sue, Polymer, 73, 6767-6773, (2002).
[xvi]. L.N. Song, M. Xiao, X.H. Li and Y.Z. Meng, Mater. Chem, Phys., 93, 122-128, (2005).
[xvii]. D. Cho, S. Lee, G. Yang, H. Fukushima and L.T. Drzal, Macromol. Mater. Eng, 290, 179-187, (2005).
[xviii]. X. Gao, L. Liu, Q. Guo, J. Shi and G. Zhai, Materials Letters, 59, 3062-3065 (2005).
[xix]. K.T. Lau and D. Hui, Composites Part B: Engineering, 33, 263-277 (2002).
[xx]. C. Park, Z. Ounaies, K.A. Watson, R.E. Crooks, J.G. Smith Jr., S.E. Lowther, J.W. Connell, E.J. Siochi, J.S. Harrison and T.L. St. Clair, Chem. Phys. Lett.; 364, 303 (2002).
[xxi]. J.G. Smith Jr., J.W. Connell and P.M. Hergenrother, Soc. Adv. Matl and Proc. Eng. Proc.; 46: 510 (2001).
[xxii]. R. Haggenmueller, H.H. Gommans, A.G. Rinzler, J.E. Fischer and K.I. Winey, Chem Phys Lett; 330, 219 (2000).
[xxiii]. R. Andrews, D. Jacques, M. Minot and T. Rantell, Macromol. Mater. Eng., 287(6), 395 (2002).
[xxiv]. C.H. Liu, H. Huang, Y. Wu and S.S. Fan, Appl. Phys. Lett, 84, 4248-4250 (2004).
[xxv]. P. Kim, L. Shi, A. Majumdar and P.L. McEuen, Phys. Rev. Lett. 87 (21), 215502 (2001).
[xxvi]. Y. J. Hwang, Y.C. Ahn, H.S. Shin, C.G. Lee, G.T. Kim, H.S. Park and J.K. Lee, Current Appl. Phys. article in press (2005).
[xxvii]. S.U.S. Choi, Z.G. Zhang, W. Yu, F.E. Lockwood and E.A. Grulke, Appl. Phys. Lett, 79, 2252-2254 (2001).
[xxviii]. M.A. Osman and D Srivastava, Nanotechnology, 12, 21-24 (2001).
[xxix]. Q Gong, Z. Li, X Bai, D. Li, Y. Zhao and J. Liang, Mater. Sc. Eng.A 384, 209-214 (2004).
[xxx]. E.J. Siochi, D.C. Working, C. Park, P.T. Lillehei, J.H. Rouse, C.T. Topping, A.R. Bhattacharya and S. Kumar, Composites: Part B; 35: 439, 2004.
[xxxi]. H. Huang, C. Liu, Y. Wu and S. Fan, Adv. Mater (Communications), 17, 1652-1656 (2005).
[xxxii]. S.T. Huxtable, D.G. Cahill, S. Shenogin. L. Xue, R. Ozisik, P. Barone, M. Usrey, M.S. Strano, G. Siddons, M. Shim and P. Keblinski, Nat. Mater., 11, 731-734 (2003).
[xxxiii]. Y.M. Chen and J.M. Ting, Carbon, 40, 359-362 (2002).